

# Strain-Based Design Model for FRP-Confined Concrete Columns

by N. Saenz and C.P. Pantelides

**Synopsis:** A constitutive strain-based confinement model is developed herein for circular concrete columns confined with fiber reinforced polymer (FRP) composites. A series of relationships were developed from experimental data, which facilitated the establishment of the strain-based model. The FRP-confined concrete constitutive model calculates the internal damage of the column by using the radial strain. The radial and axial strains at zero volumetric strain were used to mark the beginning of effective dilation response of the FRP composite jacket. The secant concrete modulus was used in the model and expressed as a function of the secant modulus softening rate, which depends on the ultimate radial to axial strain ratio. The experimental relationship for the ultimate radial to axial strain ratio is a function of the normalized effective confining stiffness. The secant modulus softening rate is constant throughout the plastic stress-strain response until failure. The FRP-confined concrete constitutive model evaluates the ultimate radial strain, which was related to the FRP composite effectiveness. The FRP-confined concrete model predicts the stress-strain response accurately for any normalized effective confinement stiffness.

**Keywords:** confinement; constitutive model; stress-strain relationships

## 1012 Saenz and Pantelides

**Nicolas Saenz** is a structural engineer for Walter P. Moore, Las Vegas, Nevada. He received his Ph.D. and M.Sc. from the University of Utah, and his M.E. and B.Sc. degrees from the Escuela Colombiana de Ingenieria, Colombia. His research interests include strengthening of concrete with FRP composites, and performance of concrete externally reinforced with FRP composites under extreme environmental conditions.

**Chris P. Pantelides** is a professor of civil and environmental engineering at the University of Utah. He is a member of ACI Committee 374, Performance-Based Seismic Design of Concrete Buildings. His research interests include seismic design, evaluation, and rehabilitation of reinforced concrete building and bridge construction.

### INTRODUCTION

Seismic design of reinforced concrete (RC) columns in bridges requires careful reinforcement detailing, so that potential plastic hinge regions are able to ensure reasonable plastic rotation capacity and energy dissipation. This is accomplished by enabling higher compressive stresses and strains, which develop in the compression zone before failure in large earthquakes. Moment-curvature analysis of RC columns can be performed accurately if an adequate stress-strain relationship for the FRP-confined concrete is used. Research on FRP-confined concrete circular columns has shown that use of externally applied FRP composites to concrete is very effective for improving strength and ductility capacity.

FRP composite jacketing curtails the dilation tendency of confined concrete (Mirmiran and Shahawy<sup>1</sup>), thereby controlling the extent of internal damage due to the kinematic restraint provided by the FRP composite. Furthermore, damage or loss of concrete stiffness is influenced by its microstructural properties (Pantazopoulou and Mills<sup>2</sup>), which is best represented by the amount of damage or expansion of the concrete core area resisting the axial load. Internal damage is best represented by using the radial strain to account for lateral dilation of confined concrete, and the corresponding loss of stiffness of FRP-confined concrete circular columns. Despite the clear relationship of radial strain to internal damage, stress-based FRP-confined concrete models are more common than strain-based models.

FRP-confined concrete stress-strain models are typically based on the following stress-strain philosophies: Models based on the Richart, Brandtzaeg, and Brown<sup>3</sup> stress theory; the Mander, Priestley, and Park<sup>4</sup> steel stress-based model; the Richard and Abbott<sup>5</sup> stress-strain equation; and a combination of the above along with the Pantazopoulou and Mills<sup>2</sup> concrete strain-based model. The Richart, Brandtzaeg, and Brown<sup>3</sup> stress-based model uses a mathematical expression to develop regression approximations, making it valid only for the experimental database considered. The Mander, Priestley, and Park<sup>4</sup> model is a stress-based steel model that uses an energy balance approach neglecting the lateral strain energy. The Richard and Abbott<sup>5</sup> stress-strain equation fits a polynomial approximation between two straight lines and can replicate stress-strain curves exhibiting strain softening. However, it does not provide physical insight into the confined concrete mechanical behavior. The Pantazopoulou and

Mills<sup>2</sup> strain-based concrete model determines the material stiffness and damage of the concrete core by the magnitude of the radial strain, which represents the amount of internal microcracking with respect to the initial microstructural properties of concrete. This constitutive model provides a physical and fundamental interpretation of the mechanical behavior of concrete. However, its central role in FRP-confined concrete has not been developed yet in a strain-based fundamental FRP-confinement model.

Mirmiran and Shahawy<sup>1</sup>; Spoelstra and Monti<sup>6</sup>; Moran and Pantelides<sup>7</sup>; and other researchers realized the importance of radial strain in the stress-strain relationships. However, the radial strain is used to modify stress-based models that do not represent directly the observed fundamental mechanical behavior. A constitutive strain-based model for FRP-confined circular concrete columns is developed herein, which is based on the Pantazopoulou and Mills<sup>2</sup> formulation for concrete and experimental relationships for FRP-confined concrete.

### **RESEARCH SIGNIFICANCE**

A constitutive strain-based confinement model is developed herein for circular concrete columns confined with FRP composites, where evaluation of internal damage of the column as the imposed axial strain increases is estimated by using radial strain. The authors believe that a pure strain-based confinement model is obtained, which provides physical insight into the confinement mechanical behavior.

### **FUNDAMENTAL BEHAVIOR OF FRP-CONFINED CONCRETE**

The typical uniaxial stress-strain behavior of concrete circular columns confined by transverse FRP composite reinforcement is shown in Figure 1. Figure 1a describes the overall stress versus axial and radial strain response to monotonically increasing axial compressive strain, induced under displacement control. Figure 1b describes the axial strain versus radial strain relationship in which the sign convention used is that compressive stress and strain are positive and tensile radial strain is negative. Figure 1c shows the volumetric strain  $\varepsilon_v$  of Eq. (1) versus axial strain,

$$\varepsilon_v = \varepsilon_c + 2\varepsilon_\theta \quad (1)$$

where  $\varepsilon_c$  = axial compressive strain; and  $\varepsilon_\theta$  = radial strain. From Figure 1, three stress-strain regimes are identified.

#### **Linear Elastic Response Regime**

The initial response of FRP-confined concrete follows a similar behavior to unconfined concrete since radial expansion of the concrete core is insignificant (Mirmiran and Shahawy<sup>1</sup>; Xiao and Wu<sup>8</sup>) and the FRP composite jacket does not change substantially the column stiffness. As the imposed axial strain increases, microcracking of the concrete core starts to accumulate and radial strain increases faster than axial strain. Therefore, the nonlinear response deviates from elastic theory. This regime is valid for a radial strain range  $0 \leq |\varepsilon_\theta| \leq |\varepsilon_{\theta,cr}|$  and corresponding axial compression strain

## 1014 Saenz and Pantelides

range  $0 \leq \varepsilon_c \leq \varepsilon_{c,cr}$ . It is limited by initiation of microcracking in the concrete, which occurs at a radial strain of  $\varepsilon_{\theta,cr} = -0.1$  mm/m (Saenz<sup>9</sup>). Consequently, in the linear elastic response regime the stress-strain response can be calculated using Eqs. 2 to 5.

$$\nu_c = -\frac{\varepsilon_{\theta,cr}}{\varepsilon_{c,cr}} \quad (2)$$

$$\varepsilon_v = (1 - 2\nu_c) \varepsilon_c \quad (3)$$

$$f_c = E_c \varepsilon_c \quad (\text{MPa}) \quad (4)$$

$$E_c = 5700\sqrt{f'_c} \quad (\text{MPa}) \quad (5)$$

where  $\nu_c$  = Poisson's ratio;  $\varepsilon_{c,cr}$  = axial compressive strain at  $\varepsilon_{\theta,cr} = -0.1$  mm/m;  $f_c$  = axial compressive stress;  $f'_c$  = concrete compressive strength; and  $E_c$  = concrete modulus of elasticity. For normal weight concrete the Poisson's ratio is in the range of 0.15-0.25, which in this paper it is assumed as  $\nu_c = 0.20$ . The initial stress-strain relationship of Eq. 4 is found using Hooke's Law for the linear elastic response regime.

### Transition Regime

The second or transition regime is valid for a radial strain range  $|\varepsilon_{\theta,cr}| \leq |\varepsilon_{\theta}| \leq |\varepsilon_{\theta,vo}|$  and corresponding axial compression strain range  $\varepsilon_{c,cr} \leq \varepsilon_c \leq \varepsilon_{c,vo}$ . In this regime the FRP composite jacket starts to counteract the stiffness degradation of the concrete core in which the volumetric strain response is reversed from volumetric contraction to volumetric expansion or dilation, as shown in Figure 1c. As the imposed axial strain increases, damage starts to accumulate, thus increasing the radial expansion at a higher rate than the imposed axial strain. As a result, the initial volumetric contraction is reversed until it becomes zero, as shown in Figure 2.

The fundamental and physical stress-strain behavior within the transition regime can be described using Eqs. 6 to 8.

$$\varepsilon_{\theta} = -\nu_c \varepsilon_c - \left(\frac{1 - 2\nu_c}{2}\right) \varepsilon_{c,vo} \left(\frac{\varepsilon_c - \varepsilon_{c,cr}}{\varepsilon_{c,vo} - \varepsilon_{c,cr}}\right)^c \quad (6)$$

$$E_{sec} = E_c \frac{1}{1 + \frac{2\varepsilon_{\theta}}{\beta}} \quad (7)$$

$$f_c = E_{sec} \varepsilon_c \quad (8)$$

where  $c$  = rate of unstable volumetric growth with increasing axial compressive strain, which for normal weight concrete is approximately  $c = 2$ ;  $E_{sec}$  = secant concrete modulus, defined in Figure 3; and  $\beta$  = secant modulus softening rate.

Pantazopoulou and Mills<sup>2</sup> proposed that internal damage in the concrete could be measured by estimating the volumetric growth of concrete, or the amount of expansion

of the concrete core area resisting the uniaxial load. This concept is adopted herein to reflect quantitatively the softening resistance of FRP-confined concrete as a function of the area strain ( $\varepsilon_a = 2\varepsilon_\theta$ ), as defined in Eqs. 6 and 7. As the imposed axial strain increases, the volumetric strain becomes zero, identified as  $\varepsilon_{vo}$  in Figure 1c and Figure 2, and marks the beginning of volumetric expansion or effective dilation response of the FRP composite jacket.

### Ultimate Axial Stress-Radial Strain Regime

In the third regime, the axial stress versus radial strain behavior up to failure is controlled by the lateral kinematic restraint of the FRP composite jacket until the ultimate radial strain is reached. In terms of the axial stress versus radial strain relationship, it is mostly linear, as shown in Figure 1a. This regime is valid for a radial strain range  $|\varepsilon_{\theta,vo}| \leq |\varepsilon_\theta| \leq |\varepsilon_{\theta,u}|$ , and the corresponding axial compression strain range  $\varepsilon_{c,vo} \leq \varepsilon_c \leq \varepsilon_{c,u}$ .

This regime depends on the ultimate radial to axial strain ratio, defined in Eq. 9, which is a function of the normalized effective confining stiffness of the FRP composite jacket, defined in Eq. 10

$$\mu_p = -\frac{\varepsilon_{\theta,u}}{\varepsilon_{c,u}} = C_1 K_{je}^{-C_2} \quad (9)$$

$$K_{je} = \frac{2t_f E_f}{D f'_c} \quad (10)$$

where  $\mu_p$  = ultimate radial to axial strain ratio;  $C_1$  and  $C_2$  = experimental constants;  $K_{je}$  = normalized effective confining stiffness;  $t_f$  = total thickness of FRP composite jacket reinforcement;  $E_f$  = FRP composite tensile modulus; and  $D$  = concrete column diameter.

The significance of Eq. 9 is that knowing the ultimate radial strain of the FRP composite, which is related to the mechanical properties of the FRP composite laminate, the ultimate axial compressive strain could be calculated. In both the transition and the ultimate axial stress-radial strain regimes, the degree of damage is best represented by the amount of radial expansion of the concrete caused by microcracking. Since the FRP composite jacket is essentially a linear elastic material, the kinematic restraint of the concrete is linearly controlled by the amount of deformation in the FRP composite jacket. This is valid until failure or rupture of the FRP composite reinforcement is reached, which determines the ultimate radial strain of the FRP-confined concrete column. Therefore, Eq. 8 could again be used to calculate the ultimate compressive axial stress of the FRP-confined concrete circular column at  $\varepsilon_c = \varepsilon_{c,u}$  corresponding to  $\varepsilon_\theta = \varepsilon_{\theta,u}$ .

In order to determine the complete third stress-strain regime response, the axial stress-radial strain relationship is obtained from experiments and is found to be linear (Saenz<sup>9</sup>), as shown in Figure 4. The axial compressive stress for radial strain in the range  $|\varepsilon_{\theta,vo}| \leq |\varepsilon_\theta| \leq |\varepsilon_{\theta,u}|$  is:

## 1016 Saenz and Pantelides

$$f_c = E_{\theta,t}(\varepsilon_{\theta,vo} - \varepsilon_{\theta}) + f_{c,vo} \quad (11)$$

$$E_{\theta} = \frac{f_{cu} - f_{c,vo}}{\varepsilon_{\theta,vo} - \varepsilon_{\theta t}} \quad (12)$$

where  $f_{cu}$  = ultimate compressive axial stress;  $f_{c,vo}$  = axial stress at  $\varepsilon_{\theta,vo}$ , calculated using Eq. 8; and  $E_{\theta}$  = tangent radial modulus. Finally, the axial compressive strain can be found by using Eq. 8.

### PHYSICAL SIGNIFICANCE OF VARIABLES

The physical and experimental evaluation of variables is based on 108 FRP-confined concrete circular column tests in which epoxy and urethane resin-matrix, utilizing carbon and glass fibers were applied (Saenz<sup>9</sup>).

#### Radial and Axial Strain at Zero Volumetric Strain

The radial strain and corresponding axial strain at zero volumetric strain mark the effective dilation response of the FRP composite jacket. Pantazopoulou and Mills<sup>2</sup> found that porosity, which is an indicator of voids in the microstructure of solid concrete, as well as strain-induced damage, could be represented by radial strain dilation and secant modulus softening, as shown in Eqs. 6 and 7. The specific value of the axial strain corresponding to zero volumetric strain ( $\varepsilon_{c,vo}$  in Figure 1a) should decrease with mechanically induced loading. On the other hand,  $\varepsilon_{c,vo}$  should increase for high-strength concrete which is characterized by its low porosity. Figure 5a compares the volumetric versus axial strain for different values of  $\varepsilon_{c,vo}$ , and Figure 5b compares the corresponding stress-strain response. Both figures are calculated assuming that the other important variables are constant and are only plotted for the first and second regimes in the range  $0 \leq \varepsilon_c \leq \varepsilon_{c,vo}$ . It can be observed that the lower the value of  $\varepsilon_{c,vo}$  the lower the stress-strain response, meaning that mechanically induced cracking could accelerate the degree of internal concrete damage. Notice that in Figure 5a, the dark symbols show the exact location of  $\varepsilon_{c,vo}$  for the three values, and in Figure 5b the dark symbols show the corresponding values of axial strain, radial strain and axial stress.

Based on experimental results, the average axial strain at zero volumetric strain is found to be  $\varepsilon_{c,vo} = 2.06$  mm/m (Saenz<sup>9</sup>). This result agrees with Imran and Pantazopoulou<sup>10</sup>, who found that  $\varepsilon_{c,vo}$ , which is equal to the axial compressive strain at the corresponding peak stress  $\varepsilon_{co}$ , for unconfined concrete, was between 1.5 mm/m to 3.5 mm/m. The significance of this result is that the initial stiffness of the concrete column controls the degree of damage, until the FRP composite reinforcement jacket is fully engaged.

#### Ultimate Radial to Axial Compressive Strain Ratio

The ultimate radial to axial compressive strain ratio  $\mu_p$  defined in Eq. 9. The experimental constants  $C_1$  and  $C_2$  were found based on experiments (Saenz<sup>9</sup>) as:

$$\mu_p = 6.21 K_{je}^{-0.63} \quad (13)$$

The physical significance of this relationship is that knowing the normalized effective confinement stiffness and the ultimate radial strain  $\varepsilon_{\theta u}$ , which is a function of the FRP composite laminate mechanical properties, the ultimate axial strain can be determined. Moran and Pantelides<sup>11</sup> derived an equivalent expression by using a different set of experimental data from the literature, where experimental constants  $C_1$  and  $C_2$  in Eq. (13) were found as follows:  $C_1$  varied between 4.635 and 5.50 and  $C_2 = -0.67$ .

### **Ultimate Radial Strain**

The ultimate radial strain of the FRP-confined circular concrete column is reached when failure or rupture of the FRP composite jacket occurs. Since the FRP composite jacket is essentially a linear elastic material, the kinematic restraint of the concrete is linearly controlled by the amount of deformation in the FRP composite jacket. Based on 108 experiments of 150 x 300 mm FRP-confined concrete cylinders (Saenz<sup>9</sup>), the ultimate radial strain  $\varepsilon_{\theta u}$  was found to be smaller than the ultimate tensile strain of FRP tensile coupons  $\varepsilon_{fu}$ . Therefore,  $\varepsilon_{\theta u}$  could be expressed as:

$$\varepsilon_{\theta u} = \xi_f \varepsilon_{fu} \quad 0 \leq \xi_f \leq 1.0 \quad (14)$$

where  $\xi_f$  = FRP composite effectiveness. Based on the same experimental study, carbon-epoxy resin FRP composites have an average  $\xi_{f,CE} = 0.66$ ; carbon-urethane and glass-urethane resin FRP composites have an average  $\xi_{f,U} = 0.85$ .

### **Secant Modulus Softening Rate**

The secant modulus softening rate  $\beta$ , represents the slope of the area strain versus the normalized secant concrete modulus, as shown in Figure 6. The secant concrete modulus decreases with increasing void area ratio, meaning that the rate of change of the secant concrete modulus is applicable for the entire stress-strain response, as shown in Eq. 7 and Figure 3. This is attributed to the continuous growth of cracks with increased imposed axial compressive strains. The increase in void area ratio or area strain  $\varepsilon_a$  is limited by the ultimate radial strain as shown in Eq. (9). From Figure 7 it can be observed that  $\mu_p$  decreases as the normalized effective confining stiffness  $K_{je}$  increases. Therefore, by knowing the ultimate radial to axial compressive strain ratio  $\mu_p$  and secant modulus softening rate relationship  $\beta$ , the second and third stress-strain regimes can be described. Based on experimental results, the following expression was found (Saenz<sup>9</sup>):

$$\beta = -(3.41\mu_p + 1.44) \times 10^{-3} \quad (15)$$

The physical significance of Eq. 15 is that the rate of void area ratio or softening of the secant concrete stiffness depends on the normalized effective confinement stiffness  $K_{je}$ . The higher the value of  $K_{je}$  the smaller the ultimate radial to axial compressive strain

# 1018 Saenz and Pantelides

$\mu_p$ , and the higher the secant modulus softening rate  $\beta$ . Hence, by knowing the initial mechanical properties of the materials, the entire stress-strain curve could be described.

Figure 8 compares the theoretical stress-strain response for three different normalized effective confinement stiffness values. It is evident from Figure 8a that within the transition zone, the lower the value of  $K_{je}$  the higher is the axial compression stress. This phenomenon is the result of early FRP jacket effective dilation, which rapidly counteracts concrete stiffness degradation. Therefore, the area strain increases at a much greater rate than the imposed uniaxial strain because of the lower  $K_{je}$ . For axial strains beyond the transition zone and for a fixed axial strain, a much lower radial strain response is obtained as  $K_{je}$  increases, as shown in Figure 8b. From Figure 8c it can be observed that the lower the value of  $K_{je}$ , the more severe the internal damage in the confined concrete. In addition, for high values of  $K_{je}$ , the volumetric dilation or expansion could be reversed and volumetric contraction could be achieved once again at high axial compressive strains. This phenomenon is the result of high plastic strain ductility, meaning that the axial compressive strain increases at a higher rate than the radial strain, so that the volumetric strain defined in Eq. 1 would become positive once again. Furthermore, for high values of  $K_{je}$  the typical failure mode is a brittle-explosive type caused by the high degree of pore collapse or compaction of the porous concrete structure, and the high lateral strain confinement restraint due to the passive action of the FRP jacket.

## CONFINEMENT MODEL ASSESSMENT

Assessment of the confinement model for moderate and high normalized effective confinement stiffness  $K_{je}$  is presented in Figures 9 and 10, and compared with experimental results (Saenz<sup>9</sup>). Figure 9 shows the calculated stress-strain response for specimens with moderate normalized effective confinement stiffness ( $K_{je} = 27.2$ ); and Fig. 10 shows the calculated stress-strain response for specimens with high normalized effective confinement stiffness ( $K_{je} = 56.5$ ). For each value of  $K_{je}$  three test units are compared with the proposed confinement model. Clearly, variability of the experimental data exists when tested under the same conditions, but the confinement model captures the characteristics of the behavior in a satisfactory manner.

## CONCLUSIONS

A constitutive strain-based confinement model for FRP-confined circular concrete columns was developed, which is well suited for analysis and design because it does not depend on the level of axial stress directly. The FRP composite confined concrete stiffness and internal damage are determined from the radial strain, which represents the amount of internal microcracking with respect to the initial properties of concrete. The radial and corresponding axial strain at zero volumetric strain, mark the beginning of the effective dilation response of the FRP composite jacket. The secant modulus softening rate and ultimate radial to axial strain relationship were developed, and were found to be functions of the normalized effective confining stiffness. The ultimate radial strain of the FRP-confined concrete column is expressed as a function of



the FRP composite effectiveness. The entire stress-strain response was determined and found to be in good agreement with experiments results.

### ACKNOWLEDGMENTS

The writers acknowledge the financial support of the National Science Foundation under Grant No. CMS 0099792. They also acknowledge the assistance of Professor Lawrence D. Reaveley and graduate students at the University of Utah. The writers acknowledge Sika Corporation; Air Logistics Corporation and Eagle Precast Inc. for in-kind support.

### NOTATION

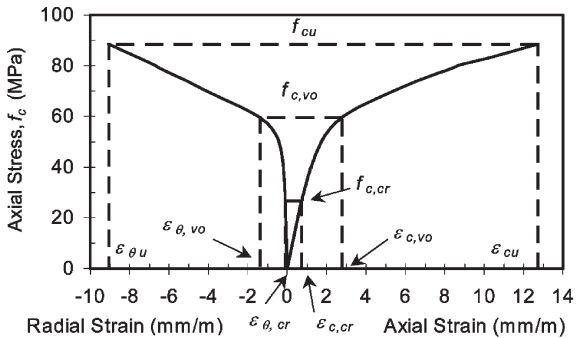
The following symbols are used in this paper:

- $c$  = rate of unstable volumetric growth
- $D$  = concrete column diameter
- $E_c$  = concrete modulus of elasticity
- $E_f$  = FRP composite tensile modulus
- $E_{sec}$  = secant concrete modulus
- $E_{\theta t}$  = tangent radial modulus
- $f'_c$  = concrete compressive strength
- $f_c$  = axial compressive stress
- $f_{c,vo}$  = axial stress at  $\varepsilon_{\theta,vo}$
- $f_{cu}$  = ultimate compressive axial stress
- $K_{je}$  = normalized effective confining stiffness
- $t_f$  = total thickness of FRP composite jacket reinforcement
- $\beta$  = secant modulus softening rate
- $\varepsilon_a$  = area strain
- $\varepsilon_c$  = axial compressive strain
- $\varepsilon_{c,cr}$  = concrete cracking axial compressive strain
- $\varepsilon_{c,vo}$  = axial strain at zero volumetric strain
- $\varepsilon_{cu}$  = ultimate axial compressive strain
- $\varepsilon_{fu}$  = ultimate FRP tensile strain
- $\varepsilon_v$  = volumetric strain
- $\varepsilon_{\theta,cr}$  = concrete cracking radial strain
- $\varepsilon_{\theta u}$  = ultimate radial strain
- $\varepsilon_{\theta}$  = radial strain
- $\varepsilon_{\theta,vo}$  = radial strain at zero volumetric strain
- $\mu_p$  = ultimate radial to axial strain ratio
- $\nu_c$  = Poisson's ratio
- $\xi_f$  = FRP composite effectiveness

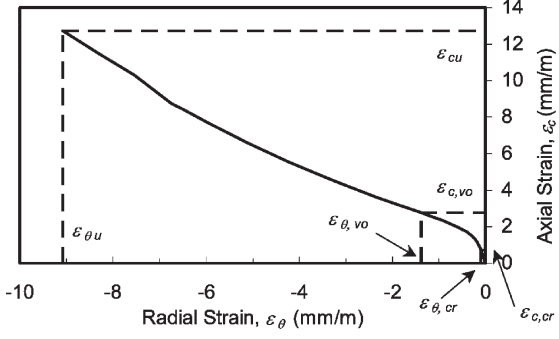
# 1020 Saenz and Pantelides

## REFERENCES

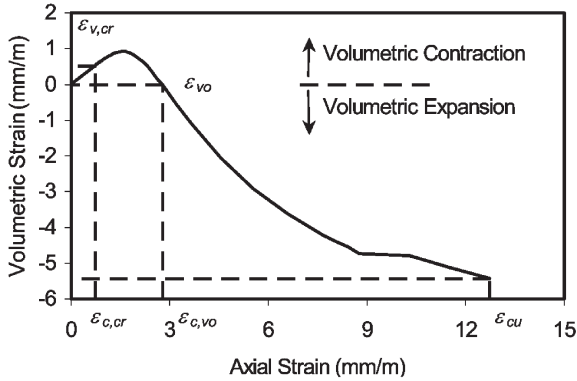
1. Mirmiran, A., and Shahawy, M. (1997), "Behavior of Concrete Columns Confined by Fiber Composites," *Journal of Structural Engineering*, ASCE, 123(5), 583-590.
2. Pantazopoulou, S. J., and Mills, R. H. (1995), "Microstructural Aspects of the Mechanical Response of Plain Concrete." *ACI Materials Journal*, 92(6), 605-616.
3. Richart, R. D., Brandtzaeg, A., and Brown, R. L. (1929), "The Failure of Plain and Spiral Reinforced Concrete in Compression." *Engineering Experiment Station Bulletin No. 190*, University of Illinois, Urbana.
4. Mander, J. B., Priestley, M. J. N., and Park, R. (1988), "Theoretical Stress-Strain Model For Confined Concrete." *Journal of Structural Engineering*, ASCE, 114(8), 1804-1826.
5. Richard, R. M., and Abbott, B. J. (1975), "Versatile Elastic-Plastic Stress-Strain Formula." *Journal of the Engineering Mechanics*, ASCE, 101(EM4), 511-515.
6. Spoelstra, M. R., and Monti, G. (1999), "FRP Confined Concrete Model," *Journal of Composites for Construction*, ASCE, 3(3), 143-150.
7. Moran, A. D., and Pantelides, C. P. (2005), "Damage-Based Stress-Strain Model for Fiber-Reinforced Polymer-Confined Concrete." *ACI Structural Journal*, 102(1), 54-61.
8. Xiao, Y., and Wu, H. (2000), "Compressive Behavior of Concrete Confined by Carbon Fiber Composite Jackets." *Journal of Materials in Civil Engineering*, ASCE, 12(2), 139-146.
9. Saenz, N. (2004), "Durability and Design of Fiber Reinforced Polymer Composites for Concrete Confinement." *Ph.D. Dissertation*, Dept. of Civil & Envir. Eng., University of Utah, Salt Lake City, Utah.
10. Imran, I., and Pantazopoulou, S. J. (1996), "Experimental Study of Plain Concrete Under Triaxial Stress." *ACI Materials Journal*, Vol. 93, No. 6, November, 589-601.
11. Moran, A. D., and Pantelides, C. P. (2002), "Variable Strain Ductility Ratio for Fiber-Reinforced Polymer Confined Concrete." *Journal of Composites for Construction*, ASCE, 6(4), 224-232.



(a)



(b)



(c)

Figure 1 — Typical stress-strain curves: (a) stress-strain; (b) axial vs. radial strain; (c) volumetric vs. axial strain

1022 Saenz and Pantelides

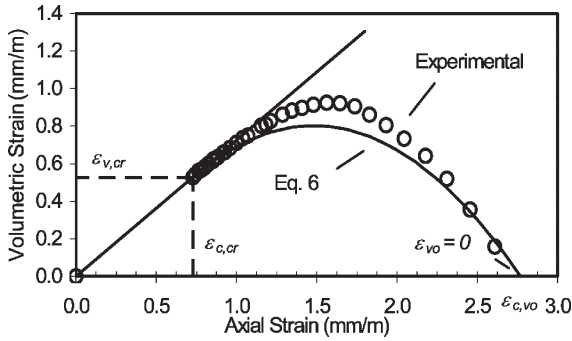


Figure 2 – Typical volumetric vs. radial strain curve

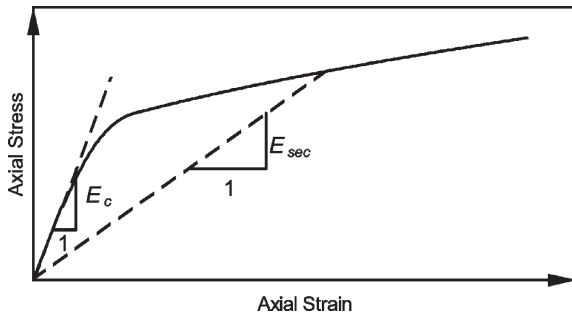


Figure 3 – Concrete modulus and secant concrete modulus definition

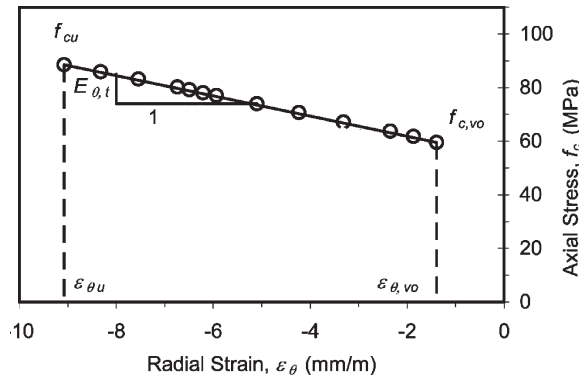


Figure 4 – Tangent radial modulus of elasticity from single test

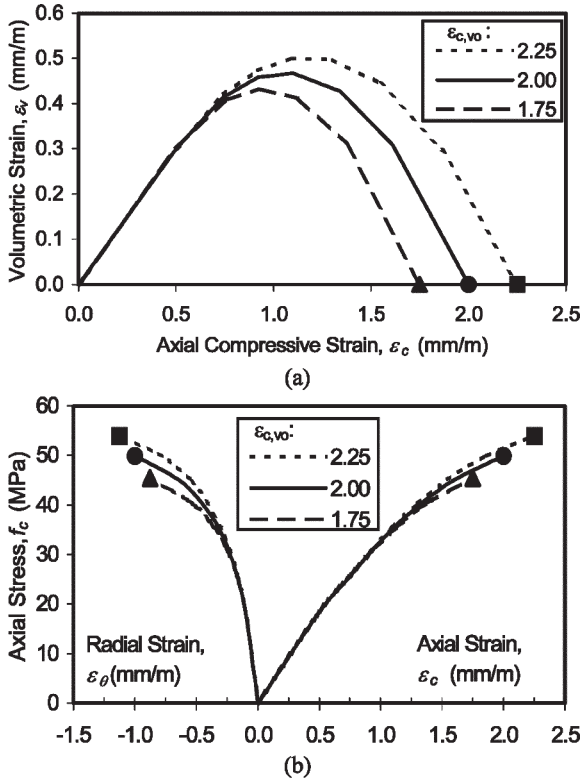


Figure 5 – Variation of axial strain at zero volumetric strain: (a) volumetric strain vs. axial strain; (b) stress-strain response

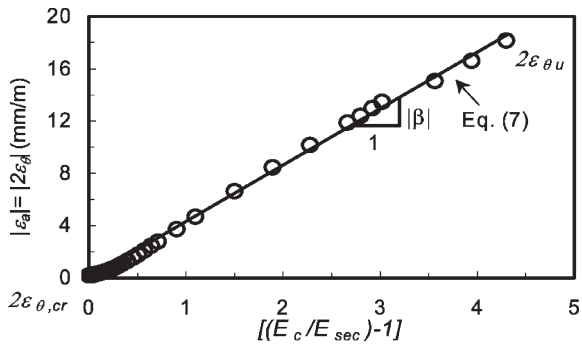


Figure 6 – Absolute area strain vs. normalized secant concrete modulus from single test

1024 Saenz and Pantelides

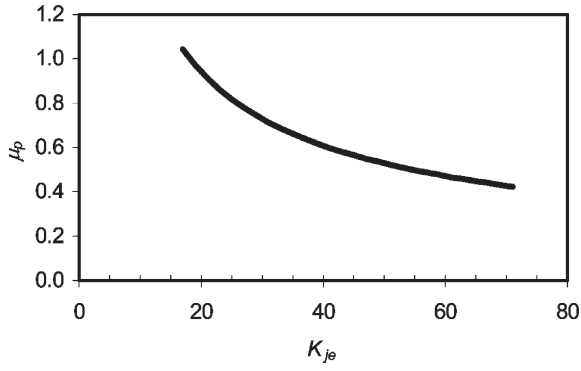
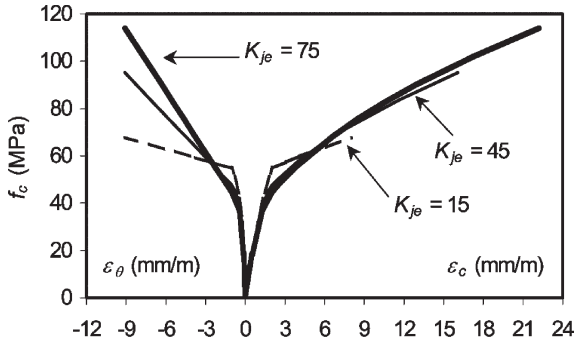
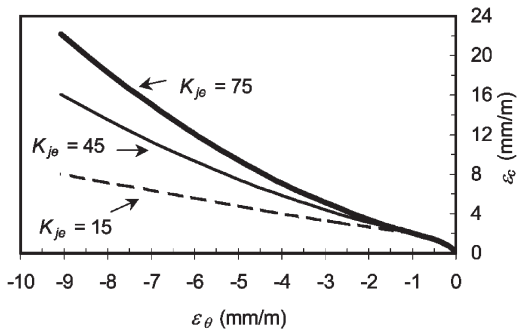


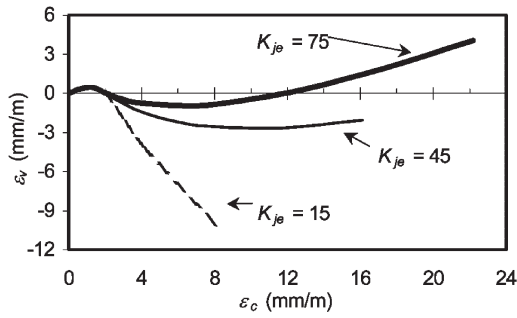
Figure 7 – Ultimate radial to axial compressive strain ratio vs. normalized effective confining stiffness



(a)



(b)



(c)

Figure 8 — Normalized effective stiffness variation response: (a) stress-strain curve; (b) axial vs. radial strain curve; (c) volumetric vs. axial strain curve

# 1026 Saenz and Pantelides

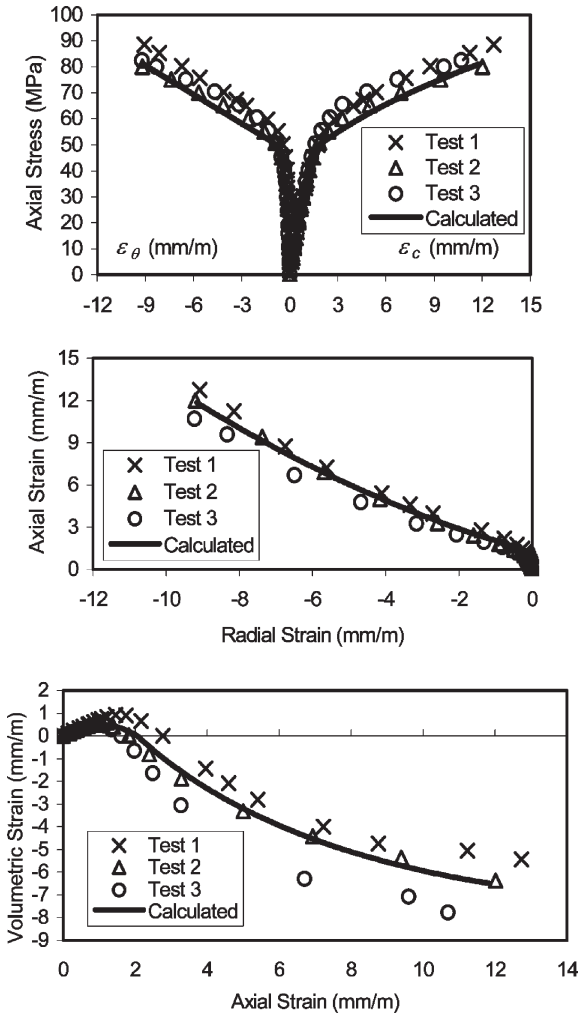


Figure 9 — Design comparison of test units with moderate effective confining stiffness,  $K_{je} = 27.2$



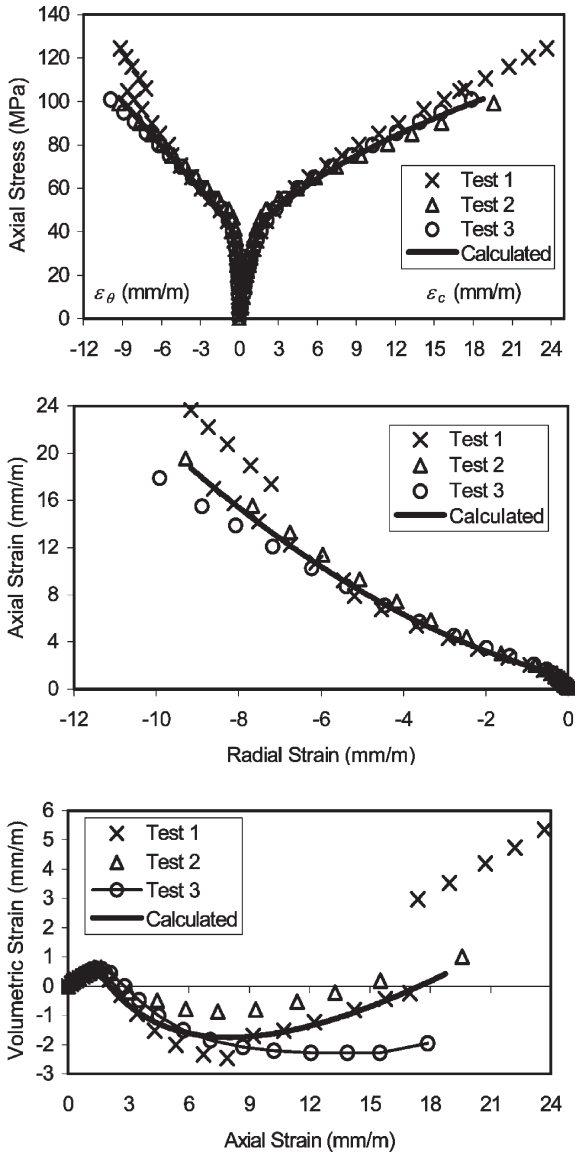


Figure 10 — Design comparison of test units with high effective confining stiffness,  $K_{je} = 56.5$

